An efficient ultrasonic-assisted bleaching strategy customized for yak hair triggered by melanin-targeted Fenton reaction

Qing Li [a,b,c,1], Zengfeng Wei [a,1], Mohan Li [d], Shiwei Li [a], Lijie Ni [a], Heng Quan [a,*], Yuyang Zhou [b,*]

[a] Hubei Key Laboratory of Biomass Fibers and Eco-Dyeing & Finishing, Wuhan Research Center of Eco-dyeing & Finishing and Functional Textile, College of Chemistry and Chemical Engineering, Wuhan Textile University, Wuhan 430200, China
[b] Jiangsu Engineering Research Center of Textile Dyeing and Printing for Energy Conservation, Discharge Reduction and Cleaner Production, National Engineering Laboratory for Modern Silk, College of Textile and Clothing Engineering, Soochow University, Suzhou 215123, China
[c] Key Laboratory of Clean Dyeing and Finishing Technology of Zhejiang Province, Shaoxing University, Shaoxing 312000, China
[d] Normal College, Eastern Liaoning University, Dandong 118003, China

A B S T R A C T

Promoting processing efficiency and taking advantage of agricultural by-products are two promising ways to achieve sustainable textile industry. This study presents a customized efficient ultrasonic-assisted bleaching strategy for yak hair – a widely existing but underexploited secondary dark shade fibre from yak. A melanin-targeted Fenton oxidation process is established which involves three phases, i.e., (I) incorporation of Fe^{2+} ions with melanin, (II) catalytic oxidative bleaching using hydrogen peroxide (H_2O_2), and (III) reductive cleansing. The bleaching efficacy, dyeing performance and tensile property of yak hair treated with and without ultrasound were explored and compared. Further, the ultrasonic bleaching mechanism in terms of the catalytic effect of Fe^{2+} ions, the promotion of H_2O_2 decomposition, removal of melanin granule from yak hair, were demonstrated. Finally, the main effects and interactions of parameters in phase II, and optimal condition were obtained through mathematical modelling based on a central composite design (CCD). Results reveal that ultrasonic bleaching dramatically enhances the whiteness index (WI) of yak hair from 11 to 45 which is 44.6% higher than those bleached without ultrasound, and also promotes the uptake of acid dyes. There is only 15% tensile strength loss and 14% elongation increment of yak hair after ultrasonic bleaching, rising from a slight damage of cuticle layer and cleavage of disulfide bonds, respectively. In the study of bleaching mechanism, Fe^{2+} ion is confirmed to improve the H_2O_2 decomposition rate by 20.9% which further runs up to 35.9% after introducing ultrasound. Ultrasound increases the concentration of hydroxyl radicals (HO•) by 94% which are the main oxidative species participating in bleaching confirmed by HO• scavenging experiment. The porous structure was observed on the cross section of yak hair stemming from the removal of melanin granules contributed by the cleaning action of ultrasound. A theoretical highest WI of 52.4 can be achieved under an optimal condition based on the CCD study. In general, the proposed melanin-targeted bleaching strategy for yak hair that integrates ultrasonic technology and Fenton reaction, is beneficial to the development of sustainable textile industry from material and processing perspectives.

1. Introduction

Recently, carbon neutrality has been increasingly emphasized, and is driving textile industry to explore alternative renewable energy and materials to pursue the goal of sustainable manufacturing. Around 8–10% of the world's carbon emissions are originated from textile industry, which directly aggravates climate change [1]. High energy and water consumption, and massive effluent discharge in conventional textile processing make it out of the criteria for sustainable industry. Promoting the processing efficiency is a facile but effective strategy for textile industry to diminish the negative impact on the environment. In addition, the resource for animal fibre (e.g., wool fibre) requires long-

Fig. 1. Proposed ultrasonic-assisted bleaching strategy for yak hair.

during specialized feeding of livestock, which indirectly but heavily impacts the global carbon emission [2]. Thus, searching for alternative fiber to reduce the consumption of conventional animal fiber is also beneficial to the environment.

Yak hair is a precious agricultural by-product for textile, showing great economy value such as fine elasticity, high tenacity, warmth, and proper moisture absorption [3,4]. Yak hair merely owns a quarter price of cashmere but with similar thermal conductivity and elasticity [5]. The global yak population reached over 15.2 million, and ca. 92% of which are bred in China (estimated by 2012) [6]. The production of fine yak hair in China is 7,060 tons per year, which is 1.6 times than that of Chinese cashmere [7]. However, yak hair still remains underutilized. One primary reason is related to the dark black colour appearance of yak hair for heat preservation and ultraviolet protection to withstand the extreme cold and UV-exposure in high altitude region [3], which greatly impacts the subsequent dyeing process, and finally limiting their final market value. The dark shade of yak hair originates from the higher content of nano/micron melanin granules than that of wool and cashmere [8,9], making the decolouration process more challenging. The conventional bleaching process to remove the natural yellowish impurities from cotton - usually undertaken at 98 °C for 60 min in alkaline, is incompatible with yak hair. Because the protein structure displays higher degradation propensity than cellulose under such harsh condition, which leads to the mechanical loss of fibre [10]. As yet, much less emphasize has been placed on the decolouration of yak hair than cotton and wool. In addition, the cuticle morphology of yak hair hinders the diffusion of oxidants thus reducing the effectiveness of bleaching. Thus, how to establish an efficient bleaching process under mild condition for yak hair before dyeing and weaving is the key challenge for the final commercialisation of yak hair.

Ultrasonic technique has been widely praised as a promising efficient and sustainable alternative method to conventional textile processing [11–14]. The compression and rarefaction generated during the ultrasonic waves propagation accounts for most physicochemical effects, which accelerate the mass transfer, swelling of fibres, and chemical reaction with less energy and time consumptions [15,16]. Apart from these advantages, it is also beneficial to textile substrates with less sacrifice of mechanical property due to milder temperature and less treatment time under ultrasound compared with conventional agitation process [17]. Especially in the present case, the advantage of ultrasound instead of physical agitation, also mitigates the mechanical loss of textile, and alleviates the entanglement between the scaled protein fibres and felting tendency of fibres [18]. To date, ultrasonic technology has been widely applied in textile wet processing including desizing, scouring, bleaching, dyeing, printing and finishing [19–23]. A numerous comprehensive studies have been carried out on the ultrasonic bleaching

of cellulose. Our previous study confirmed the higher efficiency on the scouring-bleaching of cotton/spandex fabric through a one-bath one-step ultrasonic processing than conventional method [24].

Currently, very few studies attempt to bleach yak hair using ferrous (Fe^{2+}) ions as catalyst and hydrogen peroxide (H_2O_2) - a safe and eco-friendly bleaching reagent [3,5]. The generation of reactive oxygen species (ROS) - hydroxyl radicals (HO•) from H_2O_2 is responsible for the disintegration of melanin. Such design enables a selective combination of Fe^{2+} ions with melanin rather than with keratin, because Fe^{2+} ions are preferable to be absorbed by melanin due to its higher electron density than keratin [25,26]. Such selective bleaching is assumed to reduce the damage of disulfide bonds in the un-pigmented region, however it requires further research evidence. Additionally, most bleaching methodologies are still focused on the conventional bleaching process [3]. As yet, few studies have included ultrasonic technique to the bleaching of yak hair. The ultrasonic bleaching mechanism of yak hair is still pending for investigation.

With these regards, this study introduces an efficient ultrasonic-assisted bleaching strategy customized for yak hair based on a melanin-targeted Fe^{2+}/H_2O_2 Fenton reaction. The process involves three phases, i.e., (I) complexing Fe^{2+} ions with melanin, (II) oxidative bleaching and (III) reductive rinsing to remove the ferric (Fe^{3+}) residues oxidized from Fe^{2+} ions. A batch rather than continuous ultrasonic treatment is employed considering energy saving, temperature controllability, and mechanical preservation of fibres (Fig. 1). The ultrasonic and conventional bleaching of yak fibre was compared towards a comprehensive evaluation in terms of whiteness, dyeability and tensile property. Further, the mechanism of ultrasonic bleaching was explored according to the influences of ultrasound and Fe^{2+} ions on H_2O_2 decomposition rate and HO• concentration. The cleaning action of ultrasound, and the interaction between Fe^{2+} ions and melanin granules were also studied by scanning electron microscopy equipped with energy dispersive X-ray spectroscopy (SEM-EDS). Finally, the optimal bleaching condition was obtained through mathematical modelling based on a central composite design (CCD). A biodegradable chelator − 1-hydroxy ethylidene-1,1-diphosphonic acid (HEDP) for fibre protection was introduced to the bleaching system rather than disodium ethylene diamine tetraacetate (EDTA-2Na) or diethylene triamine pentacetate acid (DTPA) [27]. Specifically, the interactions of H_2O_2, HEDP and Na_2CO_3 concentrations on the bleaching effectiveness were analysed in the CCD study.
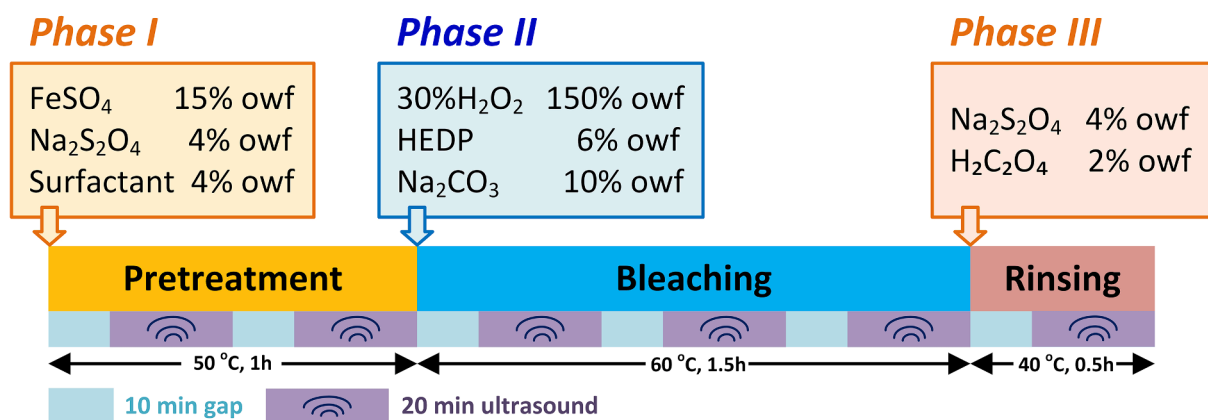
Fig. 2. Batch ultrasonic bleaching process.

Table 1
Variables and experimental design levels.

Variables (% owf)	Levels				
	-α	−1	0	1	α
A: H_2O_2	32.27	80	150	220	267.73
B: HEDP	0.95	3	6	9	11.05
C: Na_2CO_3	1.59	5	10	15	18.4

Table 2
Composition of various runs, predicted and actual responses.

Std. Order	Run Order	H_2O_2	HEDP	Na_2CO_3	WI	
					Predicted	Actual
1	5	80	3	5	15.5	16.5
2	12	220	3	5	35.4	35.0
3	4	80	9	5	12.8	13.6
4	14	220	9	5	27.7	28.0
5	18	80	3	15	30.1	30.0
6	13	220	3	15	49.6	49.0
7	20	80	9	15	30.3	30.9
8	11	220	9	15	44.7	43.9
9	1	32.27	6	10	18.8	17.5
10	3	267.73	6	10	47.7	48.7
11	10	150	0.95	10	36.8	37.0
12	9	150	11.05	10	30.4	30.0
13	15	150	6	1.59	14.5	13.6
14	6	150	6	18.41	41.1	41.8
15	2	150	6	10	44.8	45.1
16	16	150	6	10	44.8	44.1
17	19	150	6	10	44.8	43.6
18	7	150	6	10	44.8	45.0
19	17	150	6	10	44.8	45.9
20	8	150	6	10	44.8	45.3

2. Materials and methods

2.1. Materials

The yak hair fibres (Average diameter of 25 μm and length of 35 mm) and wool fibre finished product were obtained from Hebei Doveikang Auxiliary Co., Ltd., China. Surfactant polyoxyethylenated alcohols (AEO-9) was provided by Ningbo Runhe High-Tech Material Co., Ltd., China. Three acid dyes (LANASOL BLUE 3G, YELLOW 4G, SCARLET 3G) in analytical grade were purchased from Huntsman Chemical Trading (Shanghai) Co., Ltd., China. Commercial detergent specialised for wool textiles was obtained from Guangzhou Bluemoon Industrial Co. Ltd., China. Benzenepentacarboxylic acid (BA, >98%) was bought from TCI Chemical Industry Co. Ltd., China. Hydrogen peroxide (H_2O_2, 30 wt%

purity), ferrous sulfate heptahydrate ($FeSO_4·7H_2O$), sodium hydrosulphite ($Na_2S_2O_4$), sodium carbonate (Na_2CO_3), 1-hydroxy ethylidene-1,1-diphosphonic acid (HEDP), potassium permanganate ($KMnO_4$), sulphuric acid (H_2SO_4), acetate acid (HAc), sodium acetate (NaAc), oxalic acid ($H_2C_2O_4$), sodium oxalate ($Na_2C_2O_4$), sodium hydroxide (NaOH), hydroxylammonium chloride, 1,10-phenanthroline, t-butanol and dimethyl sulfoxide (DMSO) are in analytical grade. Deionized water was applied in this research.

2.2. Pre-treatment

Research on the pre-treatment of yak hair fibres with ferrous ions was carried out by discussing the effects of concentrations of $FeSO_4$ (0–20% owf) and $Na_2S_2O_4$ (0–4% owf) as well as the temperature range (30–70 °C) on whiteness of bleached fibres. (Note: owf is the weight ratio of reagent to fibre).

2.3. Bleaching

Batch ultrasonic-assisted bleaching: Yak hair fibres (1.5 g) were immersed in a mixture (50 mL) containing $FeSO_4·7H_2O$ (0.412 g), $Na_2S_2O_4$ (0.06 g) and surfactant AEO-9 (3 mL, 20 g/L) at 50 °C for 1 h (*Phase I*), washed thoroughly with 40 °C water for 3 times to remove the unfix ferrous sulphate from the fibre, and then transferred to the bleaching solution (50 mL in total) composed of 30%H_2O_2 (2.25 mL), HEDP solution (4.5 mL, 20 g/L), Na_2CO_3 solution (5 mL, 30 g/L) at 60 °C for 1.5 h (*Phase II*). The resultant yak hair fibres were rinsed with 40 °C water for 3 times to wash the residual chemical reagents. Final treatment was carried out using $H_2C_2O_4$ (0.03 g), $Na_2S_2O_4$ (0.06 g) at 40 °C for 30 min (*Phase III*). The yak hair fibres were then rinsed and dried naturally. In the above process, the mass ratio of solution against fibres was 33:1. The batch ultrasonic-assisted process was implemented using a KQ-300GDV Digital Homothermal Ultrasonic Cleaners (Ultrasonic input power, 300 W; total input power, 1050 W; ultrasonic frequency, 40 kHz; total volume, 13 L) connected to a cooling system (Kunshan Ultrasonic Instrument Co., Ltd, China). In addition, all the H_2O_2 used in this research are 30% H_2O_2 which is not further emphasized in the following text.

Conventional bleaching: Conventional bleaching was carried out in a SHZ-88A Digital Homothermal Water Bath (Changzhou Guohua Electric Appliance Co., Ltd, China) following a similar procedure as *Batch ultrasonic-assisted bleaching* described in Fig. 2, however without ultrasound.

CCD of experiment: The bleaching process (*Phase II* in Fig. 2) in terms of the concentrations of H_2O_2, HEDP and Na_2CO_3, is discussed and optimized through CCD using a statistical software package Minitab 19 (trial version, State Colleague, USA). The variable levels and codes, and
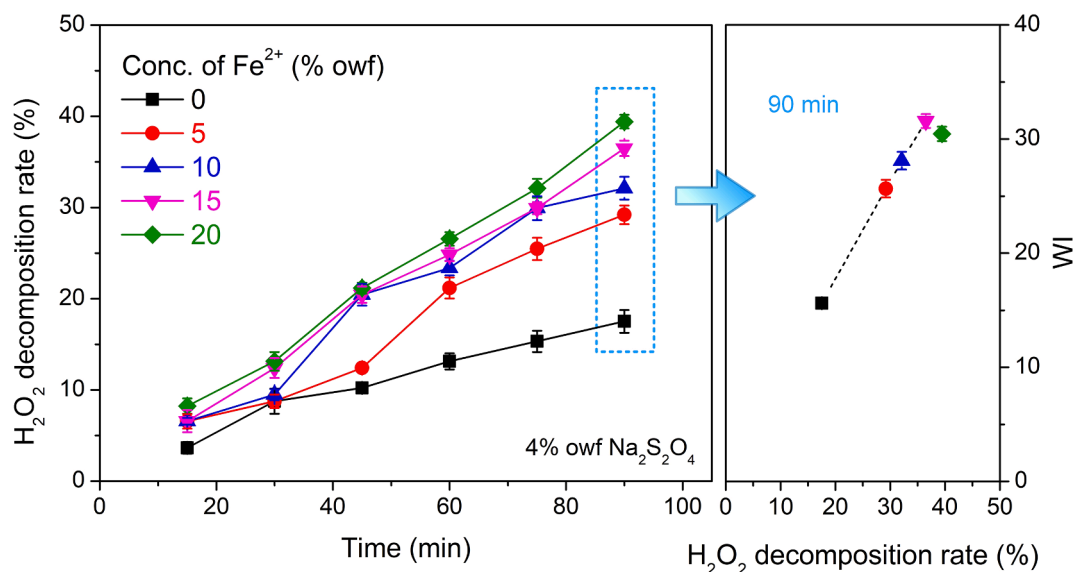
Fig. 3. H_2O_2 decomposition rate at various Fe^{2+} concentrations against time and its relationship with WI.

factorial design matrix are displayed in the Tables 1 and 2, respectively. The experiment was run randomly to decrease uncontrolled interference and repeated in triplicate. The main effect and interaction among factors were explored based on ANOVA analysis.

2.4. Dyeing

The dyeing process was implemented following a practical dyeing procedure. One gram of bleached yak hair or wool fibre was dip-dyed in a 0.2 g/L dye solution at pH 4 regulated by acetic acid. The temperature was raised from room temperature to 90 °C at a heating up rate of 5 °C/min and kept constant for 60 min. The dyed fibres were finally subjected to a rinsing process at 90 °C for 5 min using 1 g/L commercial detergent.

2.5. Characterization

2.5.1. Colour feature

The WI, apparent colour depth (K/S), lightness (L^*), redness–greenness index (a^*), yellowness–blueness index (b^*) and tristimulus values Y, Z (CIE system) of fibres were measured on a Datacolor 400 spectrophotometer using Illuminant D65 at 10∘ observe angle. A black cylindrical sample holder was used for fibres' loading to achieve a uniform thickness. The average value of ten measurements was reported. Yellowness Index (YI) was further calculated using Z and Y from the colour measurement following Eq. (1),

$$YI = 100 \times (1 - 0.847 \times Z/Y) \quad (1)$$

2.5.2. Decomposition rate of H_2O_2

The concentration of H_2O_2 in bleaching solution was determined through a standard titration procedure using $KMnO_4$ according to standard GB/T 1616-2014 – 'Hydrogen peroxide for industrial use' from which the decomposition rate of H_2O_2 was further calculated. One mL of bleaching solution at different time spot (for test), and 1 mL of the H_2O_2 solution prepared by 2.25 mL H_2O_2 (30%) and 48 mL H_2O (for reference), were added to two identical solution prepared with 10 mL of H_2SO_4 (4 mol/L) and 25 mL H_2O, respectively. These two mixtures were titrated with 0.01 mol/L $KMnO_4$ standard solution calibrated with $Na_2C_2O_4$ till faint red and stable for 30 s. The volumes (mL) of consumed $KMnO_4$ standard solution for test and reference samples were taken as V_x and V_o. The measurement was performed in triplicated and the average values were reported. The decomposition rate of H_2O_2 was calculated using Eq. (2),

$$\text{Decomposition rate of } H_2O_2 = \frac{V_0 - V_x}{V_0} \times 100\% \quad (2)$$

2.5.3. Determination of Fe^{2+} ions concentration

The Fe^{2+} ions concentration in the bleaching solution was determined based on the coloured complexing reaction between Fe^{2+} ions and 1,10-phenanthroline (Fig. S1) [28]. An absorbance/concentration relationship of 1,10-phenanthroline/Fe^{2+} chelate solution at the λ_{max} (510 nm) was established as a reference (Fig. S2). *Solution A* containing 0.024 g/L $Na_2S_2O_4$ and 0.024 g/L AEO-9 surfactant was prepared to simulate the bleaching solution. One mL of hydroxylammonium chloride solution (100 g/L), 2 mL of 1,10-phenanthroline solution (5 g/L), 5 mL of HAc-NaAc buffer solution (pH 4) and 12.5 mL *Solution A* were added into a series volumes (0.2–10 mL) of ferrous sulfate solution (Fe^{2+} ions concentration 0.025 g/L) for the measurement of UV–Vis absorption spectrum. The absorbance at 510 nm of 1,10-phenanthroline/Fe^{2+} chelate solution displayed a good linearship with a high correlation R^2 up to 0.997 indicating the high reliability for the estimation of Fe^{2+} ions concentration. Therefore, the concentration of Fe^{2+} ions in the bleaching solution and on the fibre was further calculated accordingly.

2.5.4. Determination of HO· concentration

The concentration of HO· was determined through fluorescence labelling [29]. Fluorescent probe (BA) was used to capture HO·, thus generating fluorescent hydroxyl benzenepentacarboxylic acid (BAOH) showing a maximum emission at 435 nm (Fig. S3). A F-2500 fluorescence spectrophotometer (Hitachi, Japan) with a 10.0 nm band pass slit was adopted for detection. The simulated bleaching solution containing 400 μmol/L BA, 220 μmol/L H_2O_2, 200 μmol/L HEDP and 20–120 μmol/L Fe^{2+} ions were treated using ultrasonic cleaner at 60 °C for 1 h at a pH of 10 adjusted by Na_2CO_3. For comparison, the simulated bleaching solution containing the same compositions (120 μmol/L Fe^{2+} ions) were treated using homothermal water bath under the same conditions. To explore the impact of HO· concentration on the WI of fibres, two free radical inhibitors, i.e. *tert*-butanol and DMSO were adopted to scavenge the HO·. The fibers were treated using H_2O_2 (150% owf), HEDP (6% owf), Na_2CO_3 (10% owf) at 60 °C for 1 h in the presence of 0–10 mL HO• inhibitor.

2.5.5. ATR-FTIR, XRD and SEM-EDS

The attenuated total reflectance - Fourier transform infrared (ATR-FTIR) study was implemented on a FTIR-650 spectrometer (Tianjin
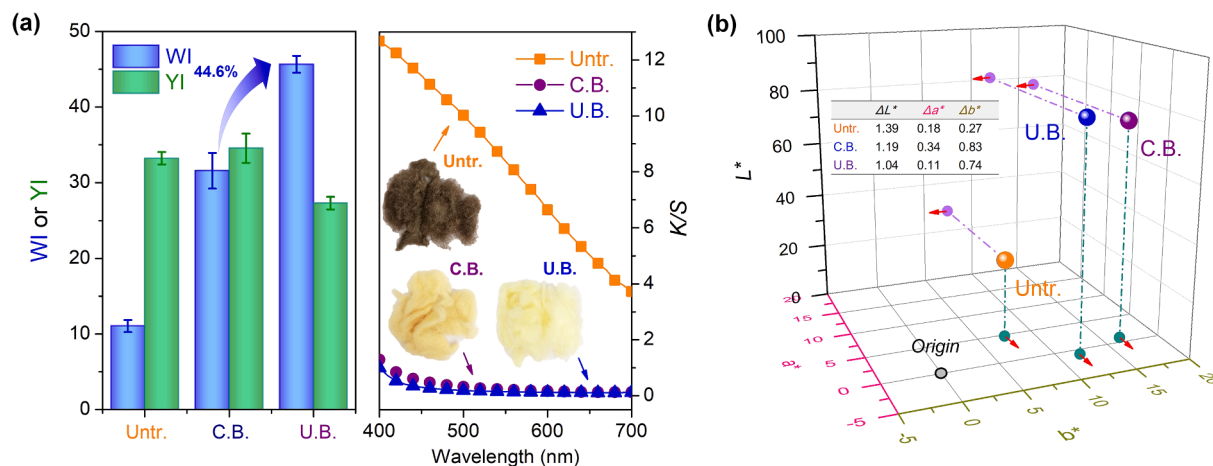
Fig. 4. (a) WI/YI and *K/S*, and (b) *L*a*b** values of untreated, conventional bleached and ultrasonic-assisted bleached yak hair fibres. (Note: Untr.: Untreated; C.B.: Conventional bleached; U.B.: Ultrasonic-assisted bleached).

Gangdong Sci. & Tech. Co., Ltd., China) conneted to a LA-100 Universal ATR accessory (Lambda Scientific Pty Ltd., Australia) in a wavenumber range of 600 to 4000 cm^{-1} at 4 cm^{-1} resolution. The crystalline structure of fibre was characterized on an Ultima IV X-ray diffractometer (Rigaku Analytical Devices, Inc. Japan) using Cu-Kα radiation (40 kV and 40 mA) with a scanning speed of 10°/min from 5° to 70°. The morphology and cross section of fibres were analysed on a JSM-IT800SHL SEM (JEOL Ltd., Japan) equipped with Energy Dispersive X-Ray Spectroscopy (EDX).

2.5.6. Tensile property

The breaking force and elongation of fibers were measured by Instron tensile tester (Model 1122) at a stretching speed of 5 mm/min with 10 mm sample length. Ten times repeated test was done on each sample. The average results were recorded.

2.5.7. Alkali-solubility

The damage of yak hair fibre by bleaching process was quantified through alkali-solubility assessment. The fibre sample (0.5 g) was dried at 105 °C for 3 h with initial mass (W_1) taken down before measurement, then placed into a 100 mL NaOH solution (0.05 mol/L) at 60 °C for 30 min, and rinsed with acetic acid and distilled water 3 times for neutralization. The mixture was finally filtrated and finally dried at 105 °C for 3 h with mass (W_2) recorded. The alkali-solubility is determined using Eq. (3),

$$G = \frac{W_1 - W_2}{W_1} \times 100\% \tag{3}$$

where W_1 and W_2 are the mass of fibres before and after alkaline treatment.

3. Results and discussion

3.1. Ferrous ion pretreatment

The concentration of Fe^{2+} ions during the pre-treatment of yak hair exerts significant impact on the bleaching efficacy related to the H_2O_2 decomposition rate, thus is explored in priority. $Na_2S_2O_4$ was also added to protect Fe^{2+} ions from oxidation. The measurement of H_2O_2 decomposition rate in this section was carried out without ultrasound. As depicted in Fig. 3, the gradual increase of H_2O_2 decomposition rate without Fe^{2+} ions indicates a mild bleaching process. However, the H_2O_2 decomposition rate in the presence of Fe^{2+} ions dramatically increased as the time proceeding, which demonstrates that the decomposition of H_2O_2 was stimulated by Fe^{2+} ions. Higher H_2O_2

decomposition rate and WI were achieved at higher Fe^{2+} ions concentration. This is due to the fact that a large quantity of reactive oxygen species (ROS) was produced, giving rise to the adequate oxidative degradation of melanin granules thus enhancing WI. The WI increased linearly against H_2O_2 decomposition rate however decreased at 20% owf of Fe^{2+} ions. This is because that a part of Fe^{2+} ions merely adsorbed on the surface of yak hair rather than on the pigment granules. The excessive Fe^{2+} ions may lead to the decomposition of H_2O_2 on the surface of fibre rather than on the colour impurities, and cause cuticle damage, thereby reducing the whiteness. In general, 15% owf Fe^{2+} ions were adopted for following experiment considering the whiteness and intrinsic nature of fibres. In addition, the temperature during Fe^{2+} pretreatment exerts marginal impact on the WI of the fibres (Fig. S4). The maximum WI was achieved at 50 °C. An increase trend of WI took place at higher $Na_2S_2O_4$ concentration and slowed down at around 4% owf, which is due to the better protection of Fe^{2+} from oxidation into Fe^{3+} (yellowish) promoting the subsequent bleaching process. Thus, 50 °C and 4% owf $Na_2S_2O_4$ was adopted for the pretreatment process.

3.2. Comparison between ultrasonic-assisted and conventional bleaching

3.2.1. Bleaching efficacy

The bleaching efficacy of yak hair fibers treated with and without ultrasound is demonstrated by their WI and YI values and else colour features (*L*a*b** and *K/S* values). As depicted in Fig. 4, untreated yak hair fiber shows a low WI around 10. The high *K/S* value and low *L*a*b** values (dots are close to origin) of fibers indicates the dull brownish apparent colour of untreated yak hair (See the inserted photo). Both conventional and ultrasonic-assisted bleaching treatment effectively improve the WI, and reduce the colour shade reflected by the dramatically decreased *K/S* and enhanced *L** values. It is worth to note that the yak hair fibers bleached under ultrasound increases in WI by 44.6% over those bleached through conventional process, which is consistent with the fact that the ultrasonic bleached fibers show lower YI and *b** than those of conventionally bleached fibers. The remarkable bleaching effect by ultrasound is attributable to the following factors. The ultrasonic cavitation effect gives rise to the generation of a numerous tiny bubbles in the bleaching solution. The high velocity jetting liquid emerged from the collapse of bubbles, accelerates the mixing function on the boundaries between fiber and solution, thereby promoting the transfer of Fe^{2+} and H_2O_2 to the fiber surface [30]. The slight relief of the cuticle scales and sufficient swelling of yak hair fiber in the ultrasonic medium is favourable for the penetration of bleaching components (Fe^{2+} and H_2O_2) to the fiber interior [31], enhancing the adsorption between Fe^{2+} and colour impurities, and increasing the H_2O_2 concentration around
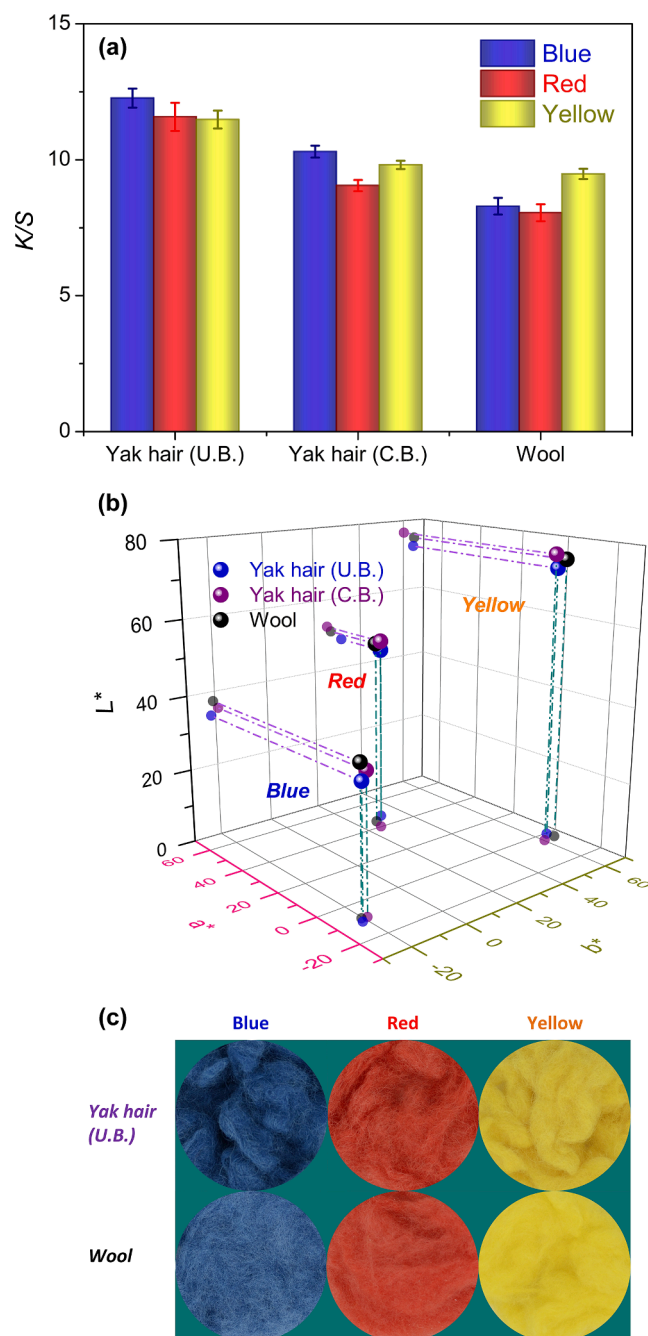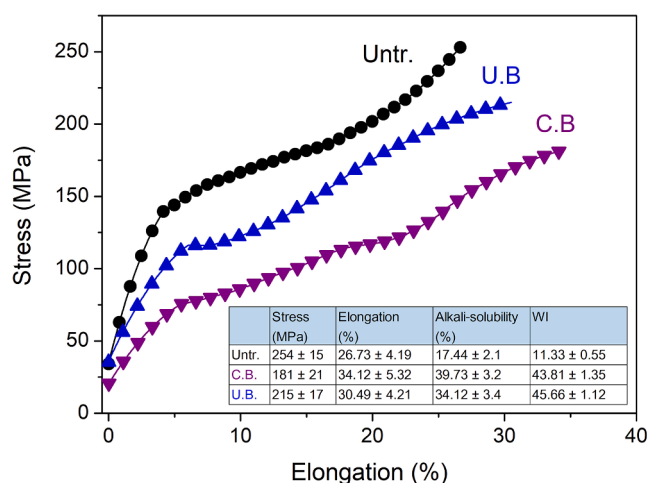
Fig. 6. Load-extension curves of yak hair fibers. (Note: Untr.: Untreated; C.B.: Conventional bleached; U.B.: Ultrasonic-assisted bleached).

treated with conventional method, which indicates a higher bleaching uniformity achieved by ultrasound. To be specific, the highly frequent compression and rarefaction of ultrasonic wave upgrades the efficiency of mass transfer in the heterogeneous solid/liquor bleaching system, thus increasing the interaction between ROS and melanin granules for a better removal of melanin granules compared with the conventional mechanical agitation. In all, the ultrasonic-assisted bleaching process is able to simultaneously increase the whiteness and decrease the yellowness of the yak hair fibre, showing superior efficacy than the conventional bleaching method.

3.2.2. Dyeing performance

The dyeing performance of the yak hair bleached with and without ultrasound was evaluated using three commercial acid dyes compared with the dyeing of wool fibres. In general, yak hair fibres after bleaching and dyeing display an equivalent or even better dyeing performance than wool fibres, which demonstrates the feasibility of yak hair for commercialization in the future. Moreover, yak hair showed high colour depth (Fig. 5a) rising from the high dye uptake (See the photos of dye solutions before and after dyeing in Fig. S5). Therein, yak hair fibres bleached under ultrasound display higher colour depth, and accordingly low $L*$ values than those without ultrasound (Fig. 5b). This is caused by the crack of yak hair cuticle outlayers and the generation of internal pores from the removal of the melanin granules, thus promoting the adsorption capability of dyes (verified in the section *3.3. Bleaching mechanism*). The yak hair fibres dyed into three primary colours (Fig. 5c) showed uniform and dark colour appearance demonstrating that they are desirable alternatives to the commercial dyed wool fibres.

3.2.3. Tensile property

Under the same condition including time, temperature and chemical usage, the protein fibre treated under ultrasound displays higher tensile loss due to the impact of ultrasonic impulse on the surface and inner structure of fibre [24]. However in the current case, it is reasonable to compare the tensile property of the yak hair samples with similar WI enhancement after ultrasonic-assisted (at 60 °C for 90 min in Phase II) and conventional (at 70 °C for 90 min in Phase II) bleaching. As depicted in Fig. 6, the tensile strength of yak hair fibres at break decreased after bleaching due to the inevitable damage of keratin structure caused by the oxidation [3,7]. Yak hair fibres also showed an increase in elongation which is attributable to the cleavage of disulfide bonds [3,7]. The results for ultrasonic-assisted and conventional bleaching are distinctive. Notably, there is less strength loss and smaller elongation increase of yak hair bleached under ultrasound than those treated by conventional method, which is consistent with the results of alkali-solubility
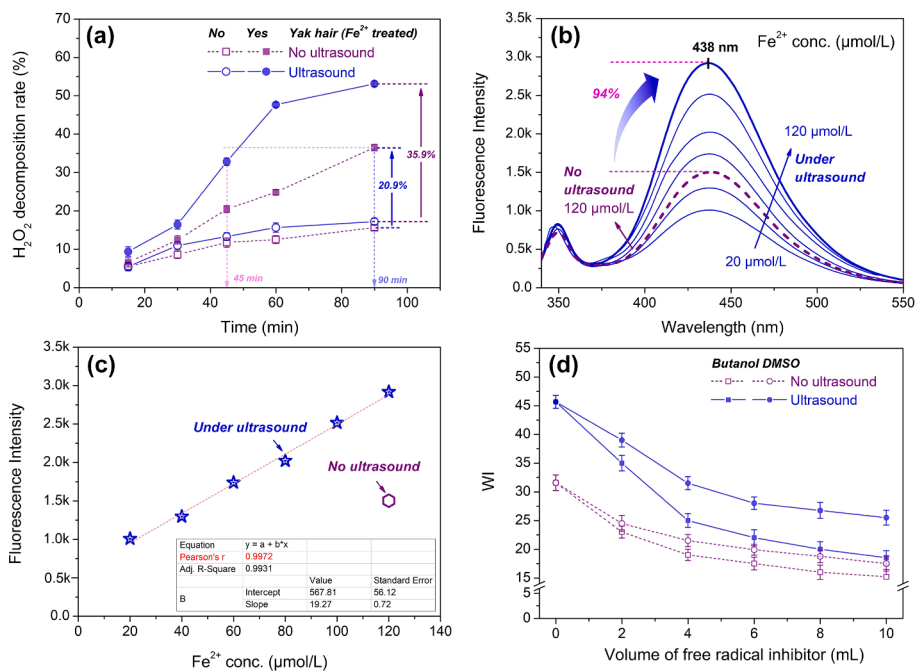
Fig. 5. (a) *K/S* and (b) *L*a*b** values and (c) photos of dyed fibres. (Note: C.B.: Conventional bleached; U.B.: Ultrasonic-assisted bleached; Standard deviation of *L*a*b** values are displayed in Table S1).

colour impurities. Meanwhile, the "hot spot" produced by the bubbles breakage induces localized high-temperature and high-pressure phenomenon. Such extreme conditions promote H_2O_2 decomposition that increases the total concentration of ROS under the catalyst effect of Fe^{2+}, and provide a greater surface accessibility to accelerate the oxidation reaction between ROS and colour impurities [32]. Those assumptions are further verified in the following section (*3.3. Bleaching mechanism*). The $a*$ values of bleached yak hair fiber are lower than untreated one, indicating the decrease of red colour shade. Conversely, the $b*$ values after bleaching increased, because the bleached fibre shows very light yellowish, which likely is the natural colour of protein fiber (See the inserted photo). The yak hair fibers bleached under ultrasound have smaller error values of WI, YI, $L*$, $a*$ and $b*$ than those

Fig. 7. Bleaching mechanism study: (a) H_2O_2 decomposition rate with and without Fe^{2+} treated yak hair and ultrasound, (b,c) HO• concentration under Fe^{2+} with and without ultrasound, (d) WI values of yak hair in the presence of free radical inhibitor, (e1,2) SEM-EDS analysis of the cross section of the Fe^{2+} treated yak hair, SEM images of the cross sections of yak hair before (f1-3) and after (f4-6) ultrasonic bleaching, SEM images of Untr. (g1), C.B. (g2) and U. B. (g3) yak hair surface. (Note: Untr.: Untreated; C.B.: Conventional bleached; U.B.: Ultrasonic-assisted bleached).
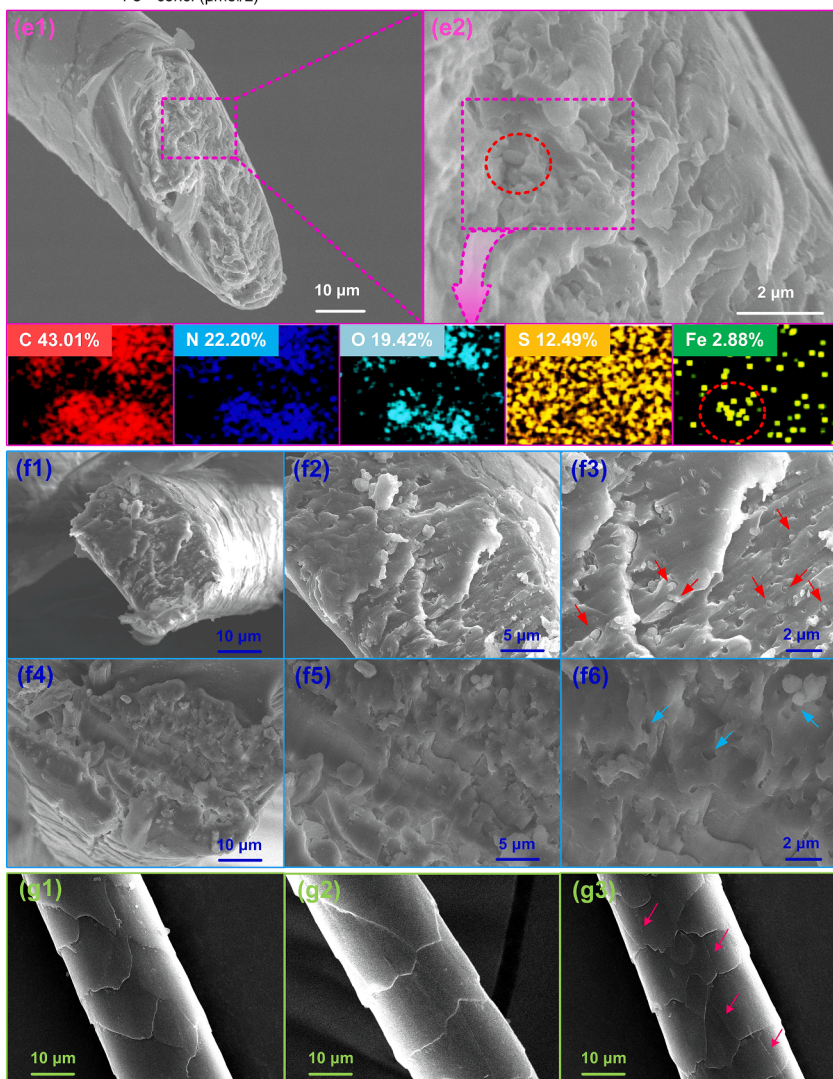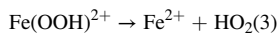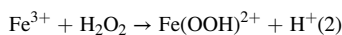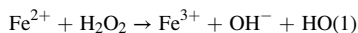
Table 3
ANOVA for the response surface quadratic model.

Source	DF	Adj SS	Adj MS	F-Value	p-Value
Model	9	2771.55	307.95	278.61	<0.001
Linear	3	1918.52	639.51	578.58	<0.001
H_2O_2	1	1012.09	1012.09	915.67	<0.001
HEDP	1	49.24	49.24	44.55	<0.001
Na_2CO_3	1	857.19	857.19	775.53	<0.001
Square	3	836.21	278.74	252.18	<0.001
$H_2O_2 \times H_2O_2$	1	242.04	242.04	218.99	<0.001
HEDP $\times$ HEDP	1	225.92	225.92	204.40	<0.001
$Na_2CO_3 \times$ Na_2CO_3	1	521.71	521.71	472.01	<0.001
2-Way Interaction	3	16.82	5.61	5.07	0.022
$H_2O_2 \times$ HEDP	1	12.70	12.70	11.49	0.007
$H_2O_2 \times Na_2CO_3$	1	0.11	0.11	0.10	0.754
HEDP $\times Na_2CO_3$	1	4.00	4.00	3.62	0.086
Error	10	11.05	1.11		
Lack-of-Fit	5	7.64	1.53	2.24	0.199
Pure Error	5	3.41	0.68		
Total	19	2782.52			
Model Summary	S	R-Sq	R-Sq (adj)	R-Sq (pred)	
	1.05170	99.60%	99.24%	97.71%	

(See inserted table). Thus to achieve equivalent whiteness on yak hair, using ultrasound shows a better fiber strength preservation compared with the conventional process due to a lower bleaching temperature which obviously diminishes the oxidative damage of fibre structure. Ultrasonic cleaning function facilitates the removal of a number of melanin particles from the bulk of fibre (verified in the section *3.3. Bleaching mechanism*), resulting in micron pores within fibres, which is another reason for the decline of tensile stress. An increased intensity of sulphoxide bond (1039 nm^{-1}) in the ATR-FTIR spectra of bleached yak hair compared with untreated fibre, confirms the damage of disulfide bond (Fig. S6a). Other characteristic bonds such as amide I (1633 nm^{-1}), amide II (1535 nm^{-1}) and amide III (1232 nm^{-1}) remain the same after bleaching. The crystallinity of yak hair showed almost no change after bleaching confirmed by their similar typical diffraction pattern of α-keratin with a prominent 2θ peak around 10° and a broad peak around 22° (Fig. S6b) [33]. Previous research proofed that ultrasonic treatment does not affect the wool crystallinity property [34,35], however may change the crystallinity of cellulosic fibres [36]. This research further confirm the ultrasonic-assisted bleaching also exert marginal impact of the crystallinity of yak hair.

3.3. Bleaching mechanism

The bleaching mechanism of the established process is dependable on the physical and chemical actions of ultrasound combining with the Fenton reaction of catalytic Fe^{2+} ions and H_2O_2. Specifically, the Fenton reaction in the present case mainly involves the following three steps [37,38],

$$Fe^{2+} + H_2O_2 \rightarrow Fe^{3+} + OH^- + HO \quad (1)$$

$$Fe^{3+} + H_2O_2 \rightarrow Fe(OOH)^{2+} + H^+ \quad (2)$$

$$Fe(OOH)^{2+} \rightarrow Fe^{2+} + HO_2 \quad (3)$$

The H_2O_2 decomposes due to its consumption during Fenton reaction and spontaneous ionization under alkali conditions. Hydroxyl radicals (HO•) and perhydroxyl ions (HO$_2^-$) are the Fenton reaction product and ionization product, respectively. Therein, the HO• converted from H_2O_2 plays the main role in the oxidation reaction accounting for the degradation of colour impurity. Thus in this section, a comprehensive study on the bleaching mechanism is implemented by exploring the impact of ultrasound and Fe^{2+} ions on the H_2O_2 decomposition during phase II and HO• concentration of simulated bleaching solution. The cross section of

ultrasonic bleached yak hair was also studied through morphological and elemental analyses to further reveal the function of ultrasound, and the interaction between Fe^{2+} ions and melanin granules.

In general, a greater quantity of H_2O_2 decomposes along with the processing time (Fig. 7a). Less than 20% H_2O_2 decomposed in the absence of Fe^{2+} pre-treated yak hair. There is also no significant difference between the solutions with and without ultrasound. Such result demonstrates that only a minority of H_2O_2 participates in the ionization. The decomposition of H_2O_2 was drastically promoted by 20.9% with the addition of Fe^{2+} treated yak hair without ultrasound, which is mainly due to the catalytic effect of Fe^{2+}ions that promotes the Fenton reaction. In contrast, the decomposition percentage of H_2O_2 was further improved to 35.9% under ultrasound, with a value at 45 min point close to that at 90 min point without ultrasound. Obviously, ultrasound accelerates the Fenton reaction in the present bleaching system. Thus, more H_2O_2 decomposed in the presence of ultrasound and Fe^{2+}, which contributes to higher concentration of oxidative bleaching species.

As described in Fig. 7b,c, the fluorescence intensity representing the concentration of HO• in the simulated bleaching solution increases nearly in a linear trend with the increasing concentration of Fe^{2+} ions, indicating the intensification of Fenton reaction trigged by Fe^{2+} ions. It is also worth noting that the ultrasound dramatically improves the HO• concentration by 94%, which implies the specific role of ultrasound in driving the Fenton reaction towards completion. Therefore, ultrasound increases the decomposition rate of H_2O_2 through Fenton reaction, facilitating the generation of HO• for pigment degradation and finally enhancing the whiteness of fibres.

In order to further verify the function of HO• during bleaching process, two inhibitors DMSO and t-butanol are introduced to the bleaching bath to scavenge the HO• merely from solution, and both from solution and the surface of catalysts (i.e. Fe^{2+} mordanted melanin granule), respectively [24,37,39]. The relationship between the inhibitor concentration and the WI of yak hair is further established. As depicted in Fig. 7d, the WI of yak hair bleached with or without ultrasound, decreased gradually at higher inhibitor dosage, confirming the bleaching function of HO•. The WI approaches to an equilibration at a concentration of 8 mL, which indicates that most of the HO• was scavenged by the inhibitors. A larger descending trend of the curve under ultrasound than conventional method is observed, which demonstrates that more HO• was generated under ultrasound due to the accelerated decomposition of H_2O_2, which is one reason related to the enhanced WI of yak hair by ultrasonic bleaching. Compared with DMSO, a larger decline of WI was observed than the presence of t-butanol. This result indicates that the ultrasound enhances the HO• concentration both in the bleaching solution and on the surface of mordanted melanin granule.

The postulation i.e. the anchor of Fe^{2+} ions by melanin, is further verified by SEM-EDS analysis (Fig. 7e). The SEM image of the cross section of yak hair fibre shows that the melanin granules irregularly embedded in the keratin fibrils. The SEM-EDS mapping reveals that the combination of Fe^{2+} ions with the melanin granules, leaving fewer Fe^{2+} ions distributed on the rest area. The selectively anchoring of Fe^{2+} ions to the melanin granules is attributable to their strong chelating effect through multipoint combination [26,40,41]. Such mechanism not only enhances the effectiveness of the catalytic effect of Fe^{2+} ions, but also decreases the negative impact of over-oxidation on the non-coloured region of fibers which benefits for their mechanical preservation. There is an interesting finding displayed in Fig. 7f. A number of melanin granules (indicated by red arrows) were removed from the bulk of fiber, leaving micron pores (indicated by blue arrows) after bleaching due to the physical cleaning action of ultrasound. Such phenomenon also enhances the dyeing property of yak fiber shown in Fig. 5. In addition, a larger number of micro-cracks on the scale of yak hair bleached through ultrasonic than conventional methods were observed (Fig. 7g2,3), however which did not occur on the untreated fibre (Fig. 7g1). Similar phenomenon also occurred on the ultrasonic treated wool fibre [15,35]. The surface cracking is another reason related to the increase of dye
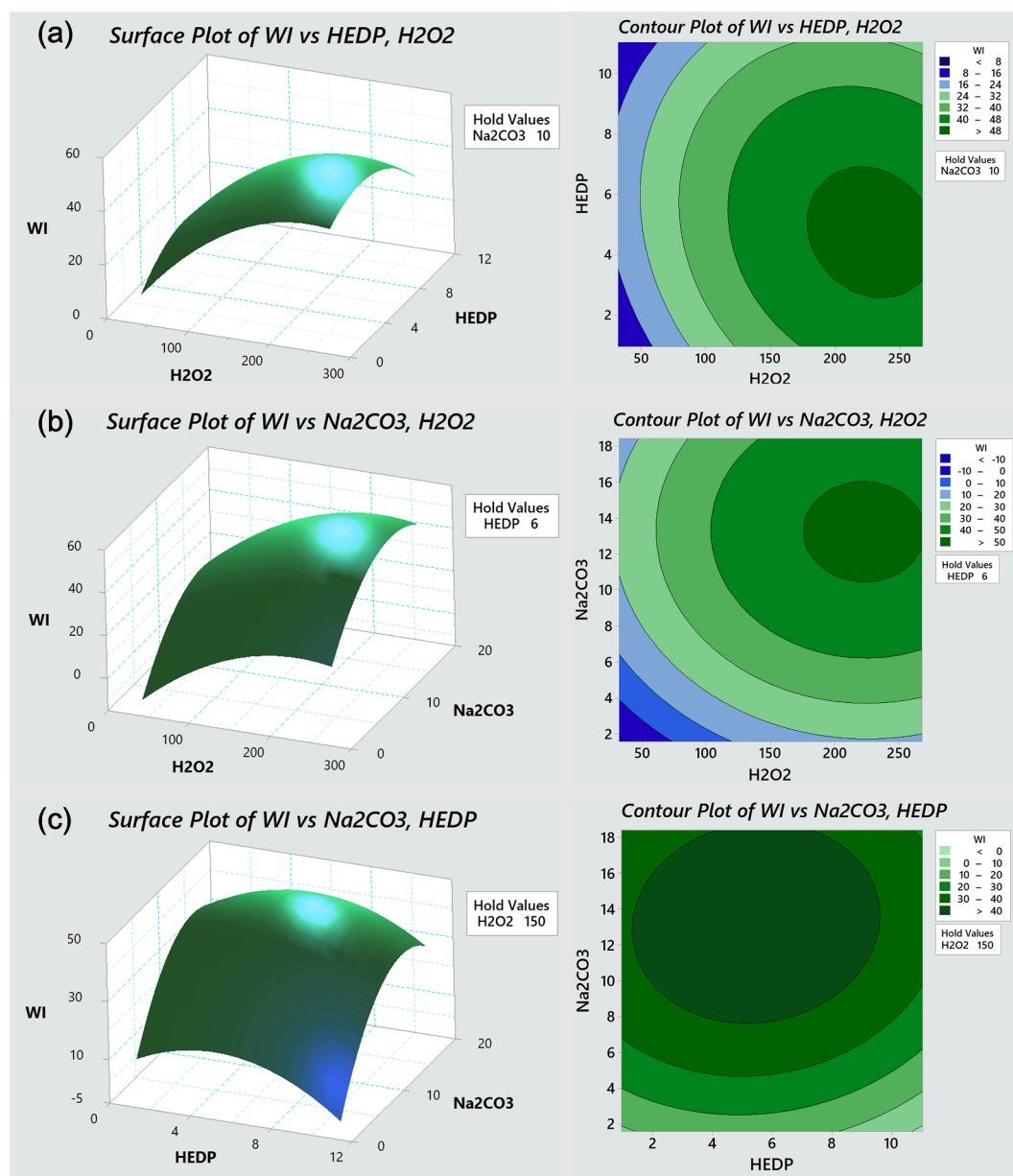
Fig. 8. Effect of variables as response surfaces and contour plots.

uptake due to the easier diffusion of dye into the fibre through the cracks as well as between the overlap of the scales [35].

As shown in Table S2, ultrasonic pretreated fiber has higher Fe content, which attributes to the promotion of adsorption and penetration of Fe^{2+} ions by ultrasound during the complexation phase (I). This is reconfirmed by the adsorptive percentage of Fe^{2+} ions during pretreatment with and without ultrasound (Fig. S7). Thus, ultrasound brings higher Fe^{2+} ions content on yak hair, which further promotes the catalytic function of Fe^{2+} ions to decompose H_2O_2 and generate $HO^{\bullet}$ for the degradation of melanin granules (see Fig. 7a,b). The O increase and S decrease imply the oxidation of disulfide bonds.

3.4. CCD optimization

3.4.1. Modelling and its corresponding ANOVA

In this section, the established ultrasonic-assisted Fenton system for yak hair bleaching (Phase II) is further investigated and optimized. In the pre-experiment of Phase II, the ultrasonic bleaching temperature and time exceeding 60 °C and 90 min respectively, leads to fiber damage

reflected by alkali-solubility (data not shown). Thus, the critical factors influencing the WI of yak hair are the concentrations of H_2O_2, HEDP and Na_2CO_3. An optimized equation and corresponding estimation of WI were achieved through mathematical modelling, which enables the determination of the parameters for research or mass production in the future. Response surface methodology (RSM) is adopted to demonstrate the relationship between variables with fewer experiments than conventional single factor method. The variables for concentrations including H_2O_2 (32.27, 80, 150, 220 and 267.73% owf), HEDP (0.95, 3, 6, 9 and 11.05% owf) and Na_2CO_3 (1.59, 5, 10, 15 and 18.4% owf) are defined as *A*, *B* and *C*, respectively. Its regression analysis by a quadratic model leads to the following equation in terms of coded factors:

$$WI = \alpha_0 + \alpha_1 A + \alpha_2 B + \alpha_3 C + \alpha_4 AB + \alpha_5 AC + \alpha_6 BC + \alpha_7 A^2 + \alpha_8 B^2 + \alpha_9 C^2$$

where *A*, *B* and *C* are variables; α_0 is the constant, α_1, α_2 and α_3 are the linear coefficients; α_4, α_5 and α_6 is the interactive coefficients; α_7, α_8 and α_9 are the quadratic coefficients.

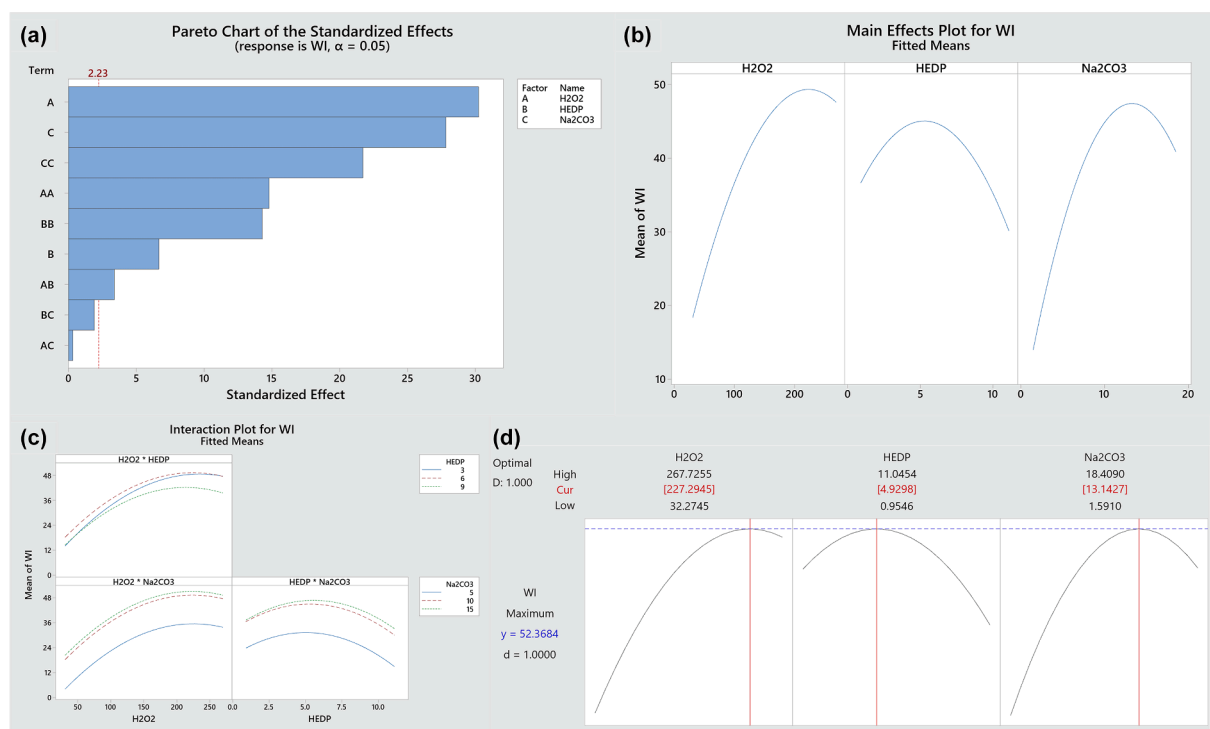Final equation in terms of actual factors:

Fig. 9. (a) Pareto chart of the standardized effects, (b) Main effects plot, (c) Interaction plot and (d) Optimization curves for WI.

$WI = -47.47 + 0.4134 \times H_2O_2 + 5.075 \times HEDP + 6.165 \times Na_2CO_3 - 0.00600 \cdot H_2O_2 \times HEDP - 0.00034 \times H_2O_2 \times Na_2CO_3 + 0.0472 \times HEDP \times Na_2CO_3 - 0.000837 \times H_2O_2^2 - 0.4399 \times HEDP^2 - 0.2406 \times Na_2CO_3^2$

The significance of the established model was assessed by ANOVA at a confidence level of 95%. The significance of each coefficient was examined by p-values those lower than 0.050 are significant whilst higher than 0.100 are not. As described in Table 3, the Model F-value of 278.61 implies the model is significant in general. The p-values of the linear coefficients (α_1, α_2 and α_3) and square term coefficients (α_7, α_8 and α_9) are smaller than 0.001, which demonstrates their significant impacts on the WI of yak hair. The p-value (0.199) for lack-of-fit far exceeds the threshold of 0.05, indicating the lack of fit is not significant. The predicted R-Sq is an indicator to elucidate the fitness of predictions from the model toward new observations, whilst R-Sq demonstrates how well the model fits the data. The high R^2 (99.60%) implies a perfect predictability for deduction using the model. There is a good closeness between the predicted and actual WI of bleached yak hair (Fig. S8). Correspondingly, the predicted R-Sq (97.71%) is close to the adjusted R-Sq (99.24%). These results demonstrate the appropriateness of using the established model for the prediction of results.

3.4.2. Interaction of variables on WI of yak hair

To further explore the effect of variables and their interactions on WI, 3D response surface and 2D contour plot were generated from the established model. As the response surface depicted in Fig. 8a, the WI increases initially at low H_2O_2 and HEDP concentrations, then approaches to a summit at c.a. 230% owf H_2O_2 and 5% owf HEDP in and decreased when both concentration increases. Accordingly, the dark green area that represents high WI value locates at the middle right region in the contour plot. Similar trends are also observed in the 3D response surfaces and contour plots in terms of H_2O_2 and Na_2CO_3 concentrations (Fig. 8b), and HEDP and Na_2CO_3 concentrations (Fig. 8c). Such phenomenon implies that there exists an optimal WI at certain concentrations of these three chemicals, and excessive usage of them could cause the decrease of WI. To be specific, the decomposition of

H_2O_2 is accelerated in the alkaline condition offered by Na_2CO_3, which is helpful to improve the WI of yak hair. However, excessively adding either or both may lead to the abrupt generation of a large number of radicals, which not only decreases the bleaching efficiency due to their self-extinction, but also induces the breakage of disulfide bonds, aggravates the degradation of keratin, and finally results in the yellowish appearance. HEDP usually plays a role of metal ion chelator to protect the fibres from over oxidation during bleaching, whereas in the current bleaching system, Fe^{2+} ions are 'preloaded' onto the yak hair combining with melanin granule (Phase I) as catalyst for the subsequent bleaching (Phase II). Thus, too much HEDP reduces the content of Fe^{2+} ions on the yak hair, and further mitigates the catalytic effect on bleaching. In all, the result of response surfaces and contour plots demonstrates that the high WI can be achieved at appropriate concentrations of H_2O_2, Na_2CO_3 and HEDP.

The extent of influence on the WI of each variable and their interactions are studied by the main effects and interaction plots, respectively. Pareto chart is used to quantify the importance of these effects. As seen in Pareto chart (Fig. 9a) and mean effect plots (Fig. 9b), H_2O_2 and Na_2CO_3 are two significant variables, followed by HEDP. The nearly paralleled lines of $H_2O_2 \times Na_2CO_3$ and HEDP $\times$ Na_2CO_3 indicating there are almost no obvious interactions. Two cross connections occur in the figure of $H_2O_2 \times$ HEDP, revealing their interactions. Such result is consistent with the corresponding p-values of coefficients shown in Table 3. Finally, the optimal bleaching condition (227.29% owf H_2O_2, 4.93% owf HEDP and 13.14% owf Na_2CO_3) is achieved from the model with theoretical highest WI of 52.4.

4. Conclusion

This study presents an efficient ultrasonic-assisted bleaching strategy customized for yak hair through a melanin-targeted Fenton oxidation. The whiteness, dyeing performance against three representative acid dyes, and tensile property of yak hair bleached using ultrasonic and conventional processes were evaluated and compared. The bleaching mechanism was explored by comparing the H_2O_2 decomposition behaviour, HO• concentration, and morphologies and elemental

compositions of fibres treated with and without ultrasound. The H_2O_2 bleaching parameters in Phase II was explored and further optimized through CCD. Results reveal that ultrasound is effective in improving the WI of yak hair from 11 up to 45 with a minor the oxidation damage of bleached fibre and the dyeability than those bleached without ultrasound. The catalytic Fe^{2+} ions facilitate the decomposition of H_2O_2 by 20.9% and the decomposition rate is further increased to 35.9% after adding ultrasound. $HO^\bullet$ is confirmed as the main oxidative species in the bleaching system upon the addition of $HO^\bullet$ scavengers, and its concentration is significantly improved by ultrasound based on the fluorescence analysis of simulated bleaching solution. The selective anchor of Fe^{2+} ions to the melanin granules is confirmed by SEM-EDS. The porous structure on the cross section of yak hair generates after ultrasonic bleaching due to the removal of melanin granules. Based on the modelling, a theoretical highest WI of 52.4 is achieved under the optimal bleaching condition (227.29% owf H_2O_2, 4.93% owf HEDP and 13.14% owf Na_2CO_3). This study demonstrates the feasibility of the efficient ultrasonic bleaching of yak hair and contributes to the development of sustainable textile industry. Such strategy is potentially scaled up, and transferable to the mild but efficient bleaching of other natural dark protein fibres such as camel hair, sable hair, ostrich feather.

CRediT authorship contribution statement

Qing Li: Conceptualization, Methodology, Data curation, Writing – original draft. **Zengfeng Wei:** Investigation, Formal analysis, Data curation. **Mohan Li:** Formal analysis. **Shiwei Li:** Formal analysis, Data curation. **Lijie Ni:** Formal analysis, Data curation. **Heng Quan:** Methodology, Supervision. **Yuyang Zhou:** Conceptualization, Methodology, Writing – original draft, Writing – review & editing, Supervision.

Declaration of Competing Interest

The authors declare that they have no known competing financial interests or personal relationships that could have appeared to influence the work reported in this paper.

Acknowledgement

Appendix A. Supplementary data

Supplementary data to this article can be found online at https://doi.org/10.1016/j.ultsonch.2022.106020.

References

[1] K. Niinimäki, G. Peters, H. Dahlbo, P. Perry, T. Rissanen, A. Gwilt, The environmental price of fast fashion, Nat. Rev. Earth Environ. 1 (2020) 189–200.

[2] P.L. Peri, Y.M. Rosas, B. Ladd, R. Díaz-Delgado, G. Martínez Pastur, Carbon footprint of lamb and wool production at farm gate and the regional scale in Southern Patagonia, Sustainability 12 (2020) 3077.

[3] C. Liu, X. Su, X. Su, C. Xie, X. Liu, Effects of optimal mordanting on the bleaching and spinning of black yak fibres, Fibres Text. East. Eur 25 (2017) 31–36.

[4] P.M. Brock, P. Graham, P. Madden, D.J. Alcock, Greenhouse gas emissions profile for 1 kg of wool produced in the Yass Region, New South Wales: A Life Cycle Assessment approach, Animal Prod. Sci. 53 (2013) 495.

[5] D. Arildii, S. Davaasambuu, A. Bazarvaani, D. Javzandulam, Optimization of mordant bleaching of yak wool with hydrogen peroxide at low temperature, J. Nat. Fibers (2020) 1–12.

[6] J. Liu, Y. Weng, Effect of stretching slenderization treatment for microstructure of yak hair, Adv. Mater. Res. 468–471 (2012) 1231–1234.

[7] K. Yan, H. Höcker, K. Schäfer, Handle of bleached knitted fabric made from fine yak hair, Text. Res. J. 70 (2000) 734–738.

[8] W. Xie, E. Pakdel, D. Liu, L. Sun, X. Wang, Waste-hair-derived natural melanin/TiO2 hybrids as highly efficient and stable UV-shielding fillers for polyurethane films, ACS Sustainable Chem. Eng. 8 (2020) 1343–1352.

[9] M. Zoccola, N. Lu, R. Mossotti, R. Innocenti, A. Montarsolo, Identification of wool, cashmere, yak, and angora rabbit fibers and quantitative determination of wool and cashmere in blend: a near infrared spectroscopy study, Fibers Polym. 14 (2013) 1283–1289.

[10] A.J. Grosvenor, S. Deb-Choudhury, P.G. Middlewood, A. Thomas, E. Lee, J. A. Vernon, J.L. Woods, C. Taylor, F.I. Bell, S. Clerens, The physical and chemical disruption of human hair after bleaching – studies by transmission electron microscopy and redox proteomics, Int. J. Cosmet. Sci. 40 (2018) 536–548.

[11] K.M. Zia, S. Adeel, F.-U. Rehman, H. Aslam, M.K. Khosa, M. Zuber, Influence of ultrasonic radiation on extraction and green dyeing of mordanted cotton using neem bark extract, J. Ind. Eng. Chem. 77 (2019) 317–322.

[12] S. Adeel, F.u. Rehman, M.U. Iqbal, N. Habib, S. Kiran, M. Zuber, K.M. Zia, A. Hameed, Ultrasonic assisted sustainable dyeing of mordanted silk fabric using arjun (Terminalia arjuna) bark extracts, Environ. Prog. Sustainable Energy 38 (2019) S331–S339.

[13] S. Adeel, K.M. Zia, M. Abdullah, F.U. Rehman, M. Salman, M. Zuber, Ultrasonic assisted improved extraction and dyeing of mordanted silk fabric using neem bark as source of natural colourant, Nat. Prod. Res. 33 (2019) 2060–2072.

[14] S. Adeel, R. Fazalur, T. Ahmad, N. Amin, S.Z. Iqbal, M. Zuber, Role of radiation treatment as a cost-effective tool for cotton and polyester dyeing, in: M. Shahid, R. Adivarekar (Eds.), Advances in Functional Finishing of Textiles, Springer Singapore, Singapore, 2020, pp. 313–347.

[15] S.J. McNeil, R.A. McCall, Ultrasound for wool dyeing and finishing, Ultrason. Sonochem. 18 (2011) 401–406.

[16] M. Vouters, P. Rumeau, P. Tierce, S. Costes, Ultrasounds: an industrial solution to optimise costs, environmental requests and quality for textile finishing, Ultrason. Sonochem. 11 (2004) 33–38.

[17] T. Harifi, M. Montazer, A review on textile sonoprocessing: a special focus on sonosynthesis of nanomaterials on textile substrates, Ultrason. Sonochem. 23 (2015) 1–10.

[18] Q. Li, C. Ding, H. Yu, C.J. Hurren, X. Wang, Adapting ultrasonic assisted wool scouring for industrial application, Text. Res. J. 84 (2014) 1183–1190.

[19] Q. Li, N. Zhang, L. Ni, Z. Wei, H. Quan, Y. Zhou, One-pot high efficiency low temperature ultrasonic-assisted strategy for fully bio-based coloristic, anti-pilling, antistatic, bioactive and reinforced cashmere using grape seed proanthocyanidins, J. Cleaner Prod. 315 (2021), 128148.

[20] P. Altay, G. Zcan, M. Tekcin, G. Sahin, S. Celik, Comparison of conventional and ultrasonic method for dyeing of spunbond polyester nonwoven fabric, Ultrason. Sonochem. 42 (2018) 768–775.

[21] Y. Pan, C.J. Hurren, Q. Li, Effect of sonochemical scouring on the surface morphologies, mechanical properties, and dyeing abilities of wool fibres, Ultrason. Sonochem. 41 (2018) 227–233.

[22] R. Bala, J. Behal, V. Kaur, S.K. Jain, R. Rani, R.K. Manhas, V. Prakash, Sonochemical synthesis, characterization, antimicrobial activity and textile dyeing behavior of nano-sized cobalt(III) complexes, Ultrason. Sonochem. 35 (2017) 294–303.

[23] V. Gonzalez, R. Wood, J. Lee, S. Taylor, M.J. Bussemaker, Ultrasound-enhanced hair dye application for natural dyeing formulations, Ultrason. Sonochem. 52 (2019) 294–304.

[24] Q. Li, L. Ni, J. Wang, H. Quan, Y. Zhou, Establishing an ultrasound-assisted activated peroxide system for efficient and sustainable scouring-bleaching of cotton/spandex fabric, Ultrason. Sonochem. 68 (2020), 105220.

[25] A. Khishigsuren, M. Nakajima, M. Takahashi, Effects of ferrous mordanting on bleaching of camel hair, Text. Res. J. 71 (2001) 487–494.

[26] S.M. Mortazavi, S. Safi, M.K. Moghadam, M. Zamani, Bleaching of black pigmented karakul wool fibers using copper sulfate as catalyst, Fibers Polym. 15 (2014) 2297–2306.

[27] L. Hui, F. Wang, J. Pang, Z. Liu, Understanding of HEDP used as chelator in pulp bleaching, Cell. Chem. Technol. 51 (2017) 301–306.

[28] I.M. Kolthoff, D.L. Leussing, T.S. Lee, Reaction of ferrous and ferric iron with 1,10-phenanthroline. III. The ferrous monophenanthroline complex and the colorimetric determination of phenanthroline, J. Am. Chem. Soc. 72 (1950) 2173–2177.

[29] F. Si, X. Zhang, K. Yan, The quantitative detection of HO· generated in a high temperature H2O2 bleaching system with a novel fluorescent probe benzenepentacarboxylic acid, RSC Adv. 4 (2014) 5860.

[30] F. Gonçalves, V. Herrero-Yniesta, I. Perales Arce, M. Escrigas Castañeda, A. Cavaco-Paulo, C. Silva, Ultrasonic pilot-scale reactor for enzymatic bleaching of cotton fabrics, Ultrason. Sonochem. 21 (2014) 1535–1543.

[31] G.M. Nazmul Islam, G. Ke, A.N.M. Ahsanul Haque, M. Azharul Islam, Effect of ultrasound on dyeing of wool fabric with acid dye, Int. J. Ind. Chem. 8 (2017) 425–431.

[32] A. Abou-Okeil, A. El-Shafie, M.M. El Zawahry, Ecofriendly laccase–hydrogen peroxide/ultrasound-assisted bleaching of linen fabrics and its influence on dyeing efficiency, Ultrason. Sonochem. 17 (2010) 383–390.

[33] L. Xia, C. Zhang, W. Xu, K. Zhu, A. Wang, Y. Tian, Y. Wang, W. Xu, Protective bleaching of camel hair in a neutral ethanol(-)water system, Polymers 10 (2018) 730.

[34] Q. Li, C.J. Hurren, H. Yu, C. Ding, X. Wang, Thermal and mechanical properties of ultrasonically treated wool, Text. Res. J. 82 (2012) 195–202.

[35] C. Hurren, P. Cookson, X. Wang, The effects of ultrasonic agitation in laundering on the properties of wool fabrics, Ultrason. Sonochem. 15 (2008) 1069–1074.

[36] Q. Li, T. Lin, X. Wang, Effects of ultrasonic treatment on wool fibre and fabric properties, J. Text. Inst. 103 (2012) 662–668.

[37] Y. Liu, J. Li, L. Wu, D. Wan, Y. Shi, Q. He, J. Chen, Synergetic adsorption and Fenton-like degradation of tetracycline hydrochloride by magnetic spent bleaching earth carbon: Insights into performance and reaction mechanism, Sci. Total Environ. 761 (2021), 143956.

[38] L. Hou, L. Wang, S. Royer, H. Zhang, Ultrasound-assisted heterogeneous Fenton-like degradation of tetracycline over a magnetite catalyst, J. Hazard. Mater. 302 (2016) 458–467.

[39] P. Ye, M. Wang, Y. Wei, Q. Zou, A. Xu, X. Li, Mechanochemical formation of highly active manganese species from OMS-2 and peroxymonosulfate for degradation of dyes in aqueous solution, Res. Chem. Intermed. 45 (2018) 935–946.

[40] A.C. Żądło, T. Sarna, Interaction of iron ions with melanin, Acta Biochim. Pol. 66 (2019) 459–462.

[41] A. Mavridi-Printezi, M. Guernelli, A. Menichetti, M. Montalti, Bio-applications of multifunctional melanin nanoparticles: from nanomedicine to nanocosmetics, Nanomaterials 10 (2020) 2276.